ISSN: 2321-7871 IMPACT FACTOR : 4.4162(UIF) VOLUME - 5 | ISSUE - 11 | 14 SEPTEMBER - 2017

WEEKLY SCIENCE

"SYNTHESIS AND STUDY OF TRANSITION METAL DOPED TITANIUM DIOXIDE NANOPARTICLES"

S. B. Deshmukh[1] , M. G. Bhosale[1] and D.V. Mane[2]
[1]Department of Chemistry, Ramkrishna Paramhansa Mahavidyalaya, Osmanabad. (Maharashtra)
[2]Department of Chemistry, Dr. Babasaheb Ambedkar Marathwada University, Aurangabad. (Maharashtra)

ABSTRACT:

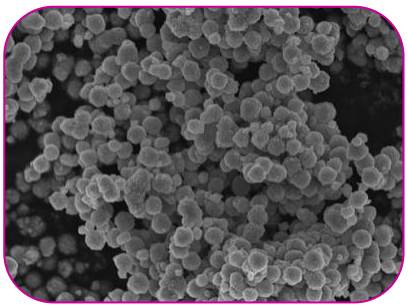

Iron doped titanium nanoparticles have been synthesized by sol-gel method using chemical bath containing appropriate volume ratio of titanium isopropoxide, oleic acid as a capping agent, conc. HNO_3, ferrous ammonium sulphate; kept at temperature of 60^0C. Synthesized nanoparticles were characterized by X-ray diffraction (XRD), Fourier-Transorm infra-red spectroscopy (FT-IR), Optical absorption measurement, Thermogravimetric-differnential thermal analysis (TGA-DTA). Single anatase phase for iron doped titania with grain size of 18 nm showed by X-ray diffraction technique. Optical absorption measurement revealed red-shift for iron doped titania nanoparticles with optical band gap value at 2.88 eV. Fourier-Transorm infra-red spectroscopy results confirmed bending vibrations of the Ti-O-Ti bond of anatase titania. The weight loss of materials were studied using TGA technique.The photocatalytic performance of synthesized material was tested for degradation of dye Rhodamine G.

KEYWORDS : *sol-gel method , thermal analysis , TGA technique.*

1. INTRODUCTION:

In the current years, scaling optical and electronic properties of nanomaterials, which become strongly size dependantalertnotice on the research of nanoparticle semi-conductors[1]

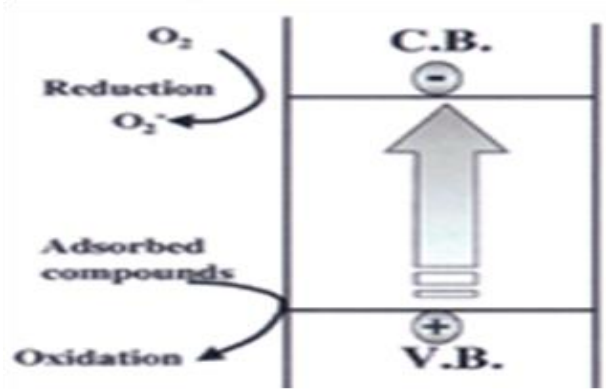

Figure 1: Schematic diagram of energy band gap of TiO_2

Strong oxidation and reduction power of photoexcited titanium dioxide (TiO_2) was realized from the innovation of Honda-Fujishima effect. In 1972, Fujishima*et al.* [2] Titanium dioxide has usualgreatconcentration becauseof its excellent optical, electrical, mechanical, and catalytic properties,which propertiesare due to chemical and biological inertness, non-toxicity, strongoxidizing/reducing power, cost-effectiveness and long-term strength against photo corrosion and chemical corrosion [3] TiO_2 shows relatively high reactivity and chemical stability under ultraviolet light (λ<387nm), whose energy exceeds the

band gap of 3.3 eV in the anatase crystalline phase. The development of photocatalysts exhibiting high reactivity under visible light ($\lambda > 400$ nm) should allow the main part of the solar spectrum, even under poor illumination of interior lighting, to be used. Several approaches for TiO_2 modification have been proposed: metal-ion implanted TiO_2 (using transition metals: Cu, Co, Ni, Cr, Mn, Mo, Nb, V, Fe, Ru, Au, Ag, Pt) [4-6]Three types of TiO_2 are abundant in nature: anatase, rutile and brookite. Anatase and rutile have photocatalytic activity. Anatase has a band gap of 3.2 eV and for rutile it is 3.0 eV. Anatase has been found to be the most active form. However, pure TiO_2photocatalyst is active under ultraviolet due to its wide band gap energy.With energy provided larger than the band gap, the electron(e^-)/hole(h^+) pairs are generated and react with O_2 and H_2O to form superoxide anion radicals ($O_2^{\cdot-}$) and hydroxyl radicals ($OH^{\cdot}$). These oxidative species (h^+, $OH^{\cdot}$, and $O_2^{\cdot-}$) are all highly reactive. [7]The metal nanoparticles are promising catalysts due to their high surface area and unique size-dependent properties, [8] but they have not found substantial applications in complex natural product synthesis, with most examples thus far being limited to known transformations [9].

2. EXPERIMENTAL PROCEDURE

For synthesis of Iron doped titanium dioxide, sol-gel method is used.

2.1 Synthesis of iron doped titanium dioxide nanoparticles

Among various compositions of Iron doped titanium dioxide, the complete synthetic procedure for representative 5 mol % Iron doped titanium dioxide is given below.

5 ml Oleic acid was taken in 250 ml beaker & it was heated up to 393 K. 10 ml titanium (IV) tetra-isopropoxide was added drop wise into it with constant stirring. The whole solution was stirred for 5 min. After that, 200 ml distilled water was added and the slurry stirred for 60 min. Solution was filtered, slurred in 200 ml distilled water, filtered &reslurred in 200ml distilled water. Using pH meter, the pH of the solution was adjusted to 10.00 by adding ammonia solution. The slurry again stirred at 333 K for 180 min., cooled to 298 K, filtered. 0.5910 gm of ferrous ammonium sulphate was taken 500 ml distilled water and & few drop of conc.HNO_3 also added. Residue was added in above 500 ml ferrous ammonium sulphate solution. The slurry again stirred at 333 K for 180 min, cooled to 298 K, filtered, and washed with 50 ml distilled water. Finally, slightly yellowish residue was observed. Residue was dried at 373 K and calcined in air at 773 K for 300 min.; which results brownish in color for iron doped titania nanoparticles.

For synthesis of whole series of iron doped titania nanoparticles, the overall procedure were kept constant except the amount of ferrous ammonium sulphate. The amount of ferrous ammonium sulphate for other various varying mol % of iron doped titanium dioxide nanoparticles is given in the table.

Table 1:- Amount of ferrous ammonium sulphate with respect to their mol % of iron intitania host lattice.

Sr. No.	Iron (mol %)	Amount of FAS (gm)
1.	1	0.1182
2.	3	0.3546
3.	5	0.5910
4.	7	0.8274
5.	9	1.0638
6.	10	1.1820

3. RESULTS AND DISCUSSION

3.1 XRD studies The XRD patterns of iron doped TiO_2 samples were obtained by using Philips PW-1710 X-ray diffractometer with Cu Kα, line (1.54056 A^0) in the 2θ ranges from 0-100^{0}C. These patterns are shown in Figure 2.

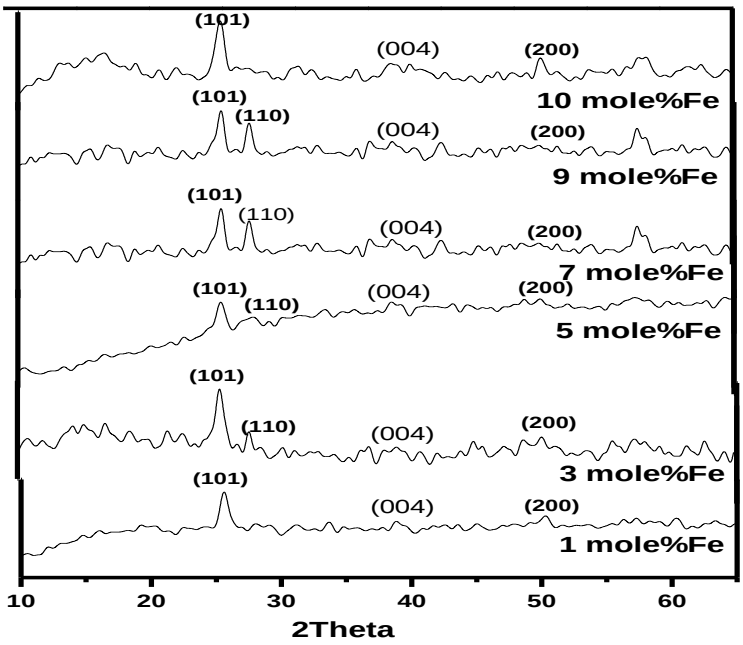

Figure 2: XRD pattern for various mole% of Fe doped TiO_2 nanoparticles

For comparative studies, the XRD pattern of anatase phase of nanotitania was used (JCPDS 21-1272). XRD studies revealed that all iron doped samples exhibit single phase anatasetitania. No peaks corresponding to oxides of iron are observed even for higher concentration of iron (10 mol %) doped samples. There is infinitesimally shift in 2θ-value as well as intensity of (101) reflection for all doped samples. This confirms the doping of iron in titania host lattice. Also, the broad hump for (101) reflection in all doped samples, confirms the formation of nanoparticles.
The grain size of samples is evaluated using Scherrer formula:

$$\text{Grain size} = 0.94 \times \lambda / \beta . \text{Cos}\theta$$

Where λ is wavelength of incident X-rays; β is the full-width at half of maxima, θ is the diffraction angle.

The observed grain size for samples is shown in following Table 2.

Sr. No.	Iron (mol %)	Grain size (nm)
1.	1	6.12
2.	3	16.00
3.	5	17.83
4.	7	20.60
5.	9	18.40
6.	10	16.58

Table 2:- Grain size with respect to their mol % of iron in titania.

3.2 FT-IR studies

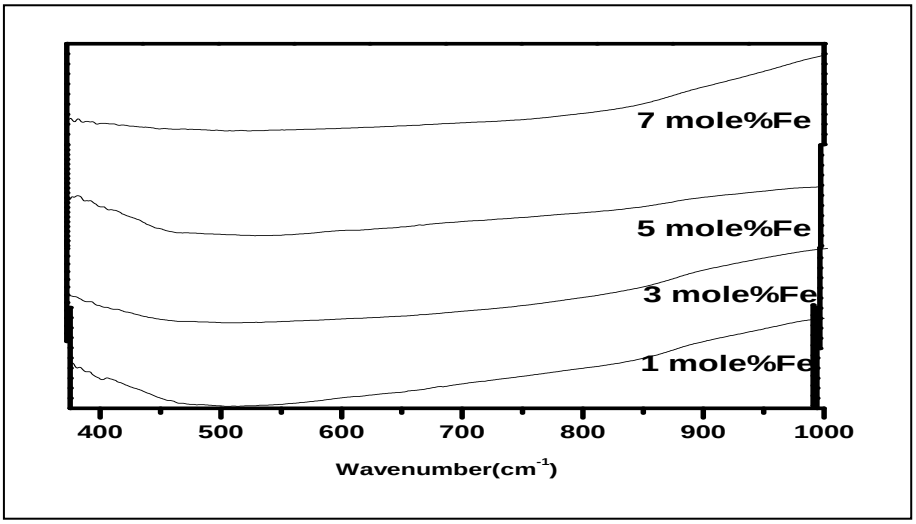

Figure 3: FT-IR Spectra of all iron doped TiO_2 samples

Figure 3 shows the IR spectra of all iron-doped TiO_2 samples. For the anatasetitania sample, the spectrum shows broad band in the 400-900 cm^{-1} region with peaks at ~460, ~515, ~694, ~778 cm^{-1}. These bands have been assigned to bending vibrations of the Ti-O-Ti bond of anatasetitania [38]. In the present investigation, the IR spectra of all samples show broad band 400-900 cm^{-1} region; which completely matches with that of anatasetitania. Taking into account of FT-IR data along with the observations obtained from XRD, it concluded that iron doped Titanianoparticles in anatase phase.

3.3 Thermogravimetric analysis (TGA)

TGA diffractogram for representative 5 mol% iron-doped titania nanoparticles shown in Figure 4. The figure indicates the mass loss in the 323 K - 723 K temperature corresponds to a loss of water, solvent and organic groups attached to material of the sample Also, the structural transition related to amorphous to anatase phase of all samples was observed in the 723 K temperature; which is clearly matches with reported elsewhere [39].

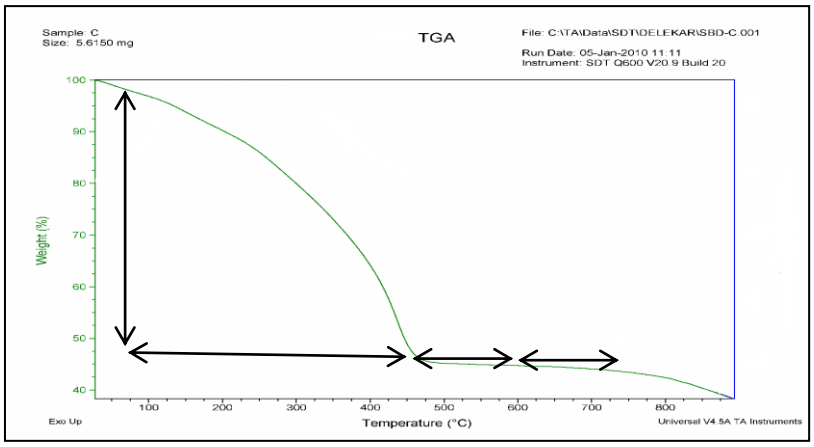

Figure 4: TGA diffractogram for representative 5 mol% iron-doped titania nanoparticles

3.4 Optical band gap measurement

Figure 5 shows the absorption spectra deduced in the ultraviolet–visible–near infrared region of electromagnetic spectrum for representative Fe–doped TiO_2 nanoparticles. In this context, it was noted that the optical absorption edge was shifted to longer wavelength from 380-530 nm upto 10 mol % of Fe–doped TiO_2 nanoparticles.

The nature of transition was determined by using the relation [40];

$$\alpha = A\,(h\nu - Eg)^n / h\nu$$

Where *h* is the Planck constant, ν is the photon frequency, *A* is a constant and *n* is an integer equal to ½ or 2. Indeed, these calculations give a relatively high absorption coefficient (α x 10^5 cm^{-1}) with direct type of transition.

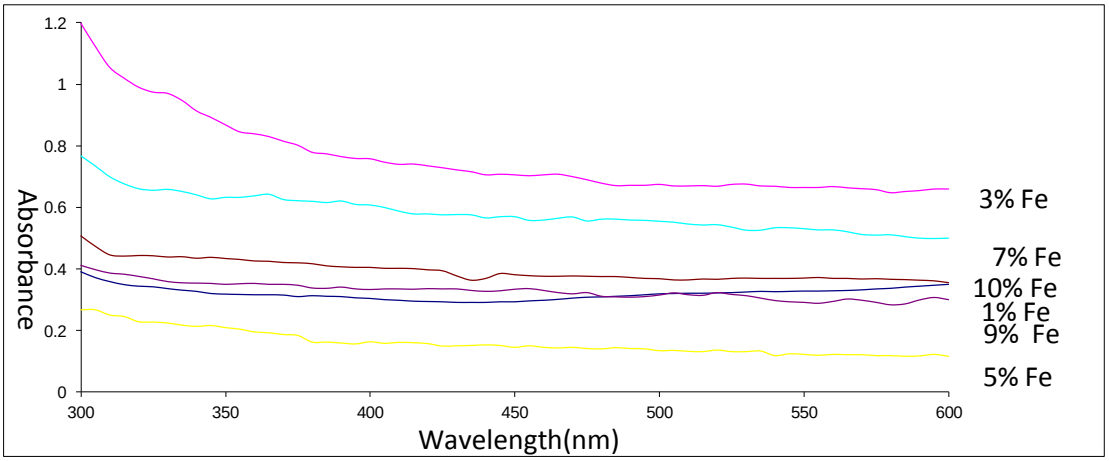

Figure 5: UV-Visible spectra of various mole% of Fe doped TiO_2 nanoparticles

This band to band direct type of transition observed for whole range of doping has been confirmed by considering plot of $(\alpha h\nu)^2$versus hν, shown in Figure 6. The energy band gap (E_g) of sample was found 2.51 ev

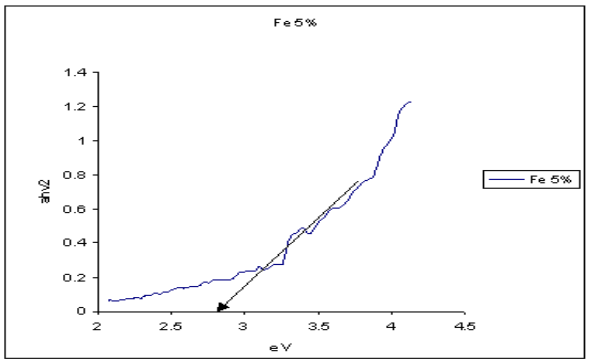

Figure 6: UV-Visible spectra converted in eV

3.5 Photocatalytic activity

Photocatalytic degradation of Rhodamine 6G (RhG)

Rhodamine6G(RhG) is a xanthene dye emitting in the red region of visible spectrum and also one of the pollutants from the textile industry; which responsible for environmental pollution and its degradation

mechanism has been studied quite well. The main absorption band of RhG at 527nmin visible region corresponds to a transition moment largely parallel to the long axis of the molecule due to$\pi \rightarrow \pi^*$ transition. Fig. 7shows absorption spectra of RhG in the suspension of 5.0 mol% Fe-doped TiO_2 nanoparticles (100 mg) at different irradiation time. As can be seen from the Fig., the maximum absorption peak at 527nm gradually decreases during the illumination. All initial absorbance disappeared after 40 min. Fig. 7shows the curve of logarithm of the remaining concentration of RhG during irradiation for 5.0 mol% Fe-doped TiO_2nanoparticles vs. irradiation time. It shows a very good linearity which indicates that the photocatalytic degradation was a first order reaction. Fig. 7shows the change of concentration of RhG in the suspension of varying iron composition in TiO_2 nanoparticlesin air atmosphere (irradiation time 420 min). It is seen that the photocatalytic degradation was fastest at 5.0 mol% iron, so all experiments were conducted at 5.0 mol% iron in TiO_2 host lattice. The result was attributed to the equilibrium of the number of surface hydroxyl on the surface of doped TiO_2 nanoparticles.

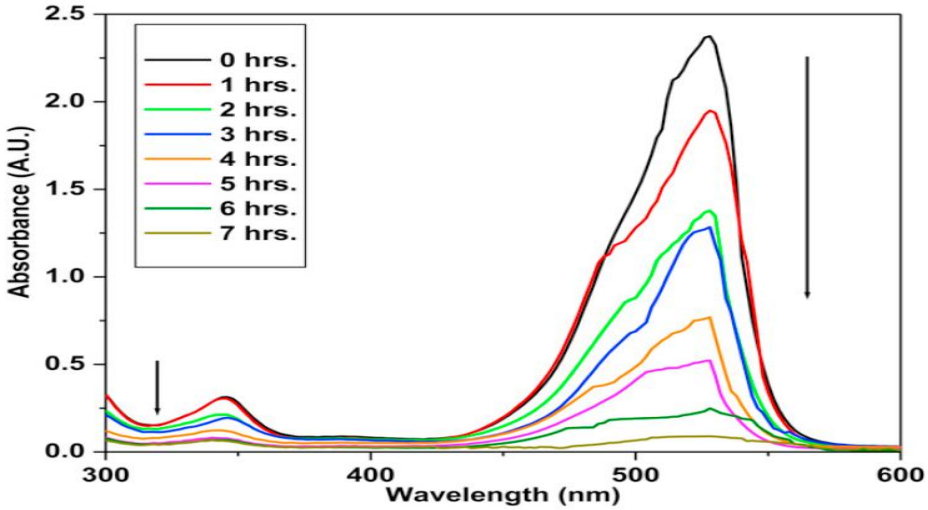

Figure 7: Absorption spectra of RhG in the suspension of 5.0 mol% Fe doped TiO_2 nanoparticles with irradiation time.

4. CONCLUSIONS

Pure anatase phase iron-doped TiO_2 nanoparticles were successfully synthesized by simple sol–gel method that allow the efficient absorption of visible light and thus enables the modifiedTiO_2 to initiate reactions effectively even under UV–vis irradiation. The effect of iron doping with different concentration (0.0–10 mole%) on the properties of TiO_2 nanoparticles was investigated from the point of view of better photocatalytic conversion efficiency. The photocatalytic efficiency of doped/undoped TiO_2 was investigated by performing the photodegradation reaction. These studies revealed that higher photocatalytic rate for 5.0 mol% Fe-doped TiO_2 nanoparticles compared with that of lower and higher Fe-doped / undoped TiO_2 nanoparticles. This significant improvement in photocatalyticperformance of 5.0 mole% Fe-doped TiO_2 nanoparticles was mainly attributed to lower band gap energy,increase in surface area and higher surfacehydroxylation group.

REFERENCES

[1]**Anpo M. (2000):** Use of visible light. Second-generation titanium dioxide photocatalysts prepared by the application of an advanced metal ion-implantation method. Pure Appl Chem; 72: 1787-1792.
[2]**Astruc, D. (2007):***Nanoparticles and Catalysis*; Wiley-VCH: Weinheim,
[3]**Fujishima A, Honda K(1972):**Electrochemical photolysis of water at a semiconductor electrode. Nature; 283: 37-38.

[4]**Fuerte MDHA, Maira AJ, Martinez-Arias A, Fernadez-Garcia M, Conesa JC, Soria J (2001):**Visible light-activated nanosized doped-TiO2 photocatalysts. ChemCommun; 24: 2718-2719.
[5]**Hoffmann M.R, Martin S.T.,Choi W,. Bahnemann D.W (1995):**Environmental applications of semiconductor photocatalysis, Chem. Rev. 95 69–96.
[6] **Henglein (1861,1989)**:A. *Chem. Re*V., *89*
[7] **M.Tomkiiewicz**(**2000**):*Catal. Today* **58** 115
[8]**X. Chen, S.S. Mao(2007) :**Chem. Rev. 107 2891–2959.
[9] **Yamashita H, Harada M, Misaka J, *et al*.(2001):** Application of ion beam techniques for preparation of metal ion-implanted TiO2 thin film photocatalyst available under visible light irradiation: Metal ionimplantation and ionized cluster beam method. J Synchrotron Rad; 8: 569-571